

Oxygen Poisoning Mechanism of Catalytic Hydrolysis of OCS over Al₂O₃ at Room Temperature

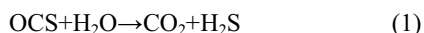
Junfeng Liu, Yongchun Liu, Li Xue, Yunbo Yu, Hong He*

State Key Laboratory of Environmental Chemistry and Ecotoxicology, Research Center for Eco-Environmental Sciences, Chinese Academy of Sciences, Beijing 100085, P. R. China

Abstract: The oxygen poisoning mechanism of the catalytic hydrolysis of carbonyl sulfide (OCS) over alumina at room temperature was investigated using *in situ* diffuse reflectance infrared Fourier transform spectroscopy (*in situ* DRIFTS), XRD, BET, and ion chromatograph (IC). The surface hydroxyl (–OH) species triggered the catalytic hydrolysis of OCS on Al₂O₃, with the formation of surface hydrogen thiocarbonate (HSCO₂[–]) species as a key intermediate. Surface SO₄^{2–} was identified with *in situ* DRIFTS and IC. It was found that the accumulation of sulfate on catalyst led to the poisoning of Al₂O₃ in the presence of oxygen.

Key Words: Carbonyl sulfide; Catalytic hydrolysis; Oxygen poisoning; Sulfate; Alumina

Carbonyl sulfide (OCS) is commonly existed in coke oven gas, coal making gas, natural gas, petroleum refining exhaust gases, the flue gas, vehicle exhaust and Claus tail gases^[1–3]. In the processes of manufacturing, OCS not only leads to corrosion of the reaction equipments but also results in the deactivation of catalysts^[3,4]. OCS can be transported into the stratosphere, where it is converted into sulfate aerosols through photooxidation, and thus it has an important impact on the environment^[5,6]. The main technologies for OCS removal include catalytic hydrolysis, oxidation conversion, and hydrogenation conversion, etc^[7]. Among these methods, catalytic hydrolysis was the most principal technology for the removal of OCS in the tail gases^[1]. Catalytic hydrolysis of OCS follows the reaction:



Recently, hydrolysis catalyst with high activity for the removal of OCS at low temperature or normal temperature has attracted considerable interest of researchers^[1,7–10]. The previous researches showed that at high temperature, the formation of elemental sulfur and sulfate on the surface of catalyst is the main reason that leads to the deactivation of catalyst for OCS hydrolysis; the higher the temperature, the faster the deactivation of catalyst^[11–14]. Alumina (Al₂O₃) is a common catalyst

carrier and activate component for the catalytic hydrolysis of OCS^[1,8–15]. Therefore, it is of great significance to study the sulfate formation mechanism of OCS over Al₂O₃ to improve the resistance of catalyst to sulfate poisoning. The catalytic hydrolysis of OCS over Al₂O₃ at room temperature has a potential in application. In this study, different crystal types of Al₂O₃ samples were chosen to investigate the hydrolysis of OCS at room temperature. The products and intermediates of OCS catalytic hydrolysis over Al₂O₃ at room temperature were inspected using *in situ* diffuse reflectance infrared Fourier transform spectroscopy (DRIFTS), ion chromatograph (IC), etc. The effects of the calcination temperature of the Al₂O₃ on the oxygen poisoning of catalyst in the catalytic hydrolysis of OCS at room temperature were studied. By combining the results of the experiments, the oxygen poisoning mechanism of the catalytic hydrolysis of OCS over Al₂O₃ was proposed.

1 Experimental

1.1 Preparation and characterization of catalyst

The samples of Al₂O₃-A, Al₂O₃-B, and Al₂O₃-C were prepared directly from boehmite (AlOOH) powder (Shandong Aluminum Corporation, China), stirred with deionized water

Received: January 2, 2007; Revised: April 5, 2007.

*Corresponding author. Email: honghe@rcees.ac.cn; Tel: +8610-62849123.

The project was supported by the National Natural Science Foundation of China (20637001, 50621804).

Copyright © 2007, Chinese Chemical Society and College of Chemistry and Molecular Engineering, Peking University. Published by Elsevier BV. All rights reserved. Chinese edition available online at www.whxb.pku.edu.cn

for 2 h, dried at 373 K for 3 h, and calcined at 573, 873, and 1473 K for 3 h, respectively. The catalyst was crushed into 20–40 meshes particles for experimental use.

The X-ray diffractometry of samples was implemented using a computerized Rigaku D/Max-II Diffractometer (Cu K_{α} radiation sources, the tube voltage of 40 kV, the tube current of 80 mA, the scanning speed of 4 ($^{\circ}$) \cdot min $^{-1}$, scanning range of 10 $^{\circ}$ –90 $^{\circ}$). The Brunauer-Emmett-Teller (BET) surface areas of the samples were obtained using Micromeritics ASAP 2010 automatic equipment.

1.2 Evaluation of the catalytic hydrolysis activity of OCS over Al₂O₃

The evaluation reactions of OCS catalytic hydrolysis over Al₂O₃ were conducted in a fixed-bed quartz reactor (ϕ 6 mm \times 150 mm). The concentrations of OCS were determined by an infrared spectroscopy (Nicolet NEXUS 670) equipped with a 2 m optical path gaseous chamber. Prior to the activity evaluation test, the Al₂O₃ catalyst samples were pretreated by heating in an oxygen flow at 373 K for 3 h. The OCS used in the experiments was the 2% OCS (OCS/N₂) standard gas (Scott Specialty Gases Inc., American). The other reactant gases were the cylinder gas, which has purity higher than 99.999%. The water vapor was introduced by N₂ pass through a water saturated generator in a water bath.

The reaction conditions were as follows: $\varphi(\text{OCS})=0.03\%$, $\varphi(\text{H}_2\text{O})=0.24\%$, $\varphi(\text{O}_2)=0, 2\%, 10\%$, balanced with N₂. The masses of the catalysts used in the activity evaluation experiments were 0.6 g, and the total gas flow rate was 100 mL \cdot min $^{-1}$ (GHSV (gas hourly space velocity) was 2500 h $^{-1}$). The reaction temperature was 298 K.

1.3 Analysis of the sulfate generated over Al₂O₃ by IC

The sulfate formed over Al₂O₃ from OCS was converted into water soluble sulfate and the quantitative analysis was determined using ion chromatograph (IC). 1.2 g of the Al₂O₃ sample was placed in the reactor, preoxidized by heating at 573 K in a 100 mL \cdot min $^{-1}$ O₂ flow gas for 3 h, cooled to 298 K, and exposed to 100 mL \cdot min $^{-1}$ 0.05% OCS + 21% O₂ flow gas for a given time. The reacted Al₂O₃ sample was washed with 100.00 mL deionized water and transported into a 500 mL dried conical flask, ultrasonically extracted for 30 min. The extracted liquid was filtered through a 0.45 μ m filter. The concentration of water soluble sulfate in the filtrated solution was analyzed by IC.

The eluant consisted of 3.5 mmol \cdot L $^{-1}$ Na₂CO₃/1 mmol \cdot L $^{-1}$ NaHCO₃ passed through the IC system (Dionex, CA) at a flow rate of 1.2 mL \cdot min $^{-1}$. The injection volume of the liquid sample was 25 μ L. The solution was filtered through a 0.2 μ m filter before entering the analytical column. The concentration of sulfate was in linear correlation with its peak area in the concentration range of 1–40 mg \cdot L $^{-1}$ ($R^2=0.9997$); thus, we can

calculate the concentration of sulfate on the basis of its peak area.

1.4 In situ DRIFTS experiment

In situ DRIFTS consists of *in situ* DRIFTS spectra apparatus equipped with a MCT detector (NEXUS670, Nicolet Co. USA), an *in situ* diffuse reflection chamber, and attachments. The component, pressure, and temperature of gas in the *in situ* diffuse reflection chamber can be precisely controlled through the mass flow controllers and a temperature controller^[16].

The procedures of catalyst preoxidized treatment are described as follows: the Al₂O₃-A sample was heated in the *in situ* infrared cell in 100 mL \cdot min $^{-1}$ O₂ at 573 K for 3 h. The Al₂O₃-B and Al₂O₃-C samples were pretreated in the *in situ* infrared cell by heating in 100 mL \cdot min $^{-1}$ O₂ at 873 K for 3 h. The prerduced treatment of catalyst: the Al₂O₃-A sample was pretreated in the *in situ* infrared cell by heating in 100 mL \cdot min $^{-1}$ H₂ at 573 K for 3 h. The reference spectrum was recorded after the pretreated sample cooled to 298 K and the absorption of water vapor was subtracted as background. The sample was exposed to 100 mL \cdot min $^{-1}$ reactant gas at room temperature, and the information of the surface species was detected using NEXUS670 *in situ* DRIFTS spectra apparatus in the wavenumber range of 650–4000 cm $^{-1}$ with 4 cm $^{-1}$ of resolution and 100 scan times.

1.5 Quantitative analysis of gas-phase OCS concentration

When the concentration of OCS gases in the IR gaseous chamber of the activity evaluation test reached an equilibrium, the integrated areas of the absorption peak of gaseous OCS located at 2071 cm $^{-1}$ and 2052 cm $^{-1}$ have a linear correlation with the concentration of OCS gas ($R^2=0.9990$) in the range of 0–0.1%, to achieve the quantitative analysis of OCS concentration.

2 Results and discussion

2.1 Sample characterization

Fig.1 shows the XRD patterns of the crude AlOOH and Al₂O₃ calcined at different temperatures. It can be seen that the Al₂O₃-A sample still exists mainly as AlOOH after the AlOOH was calcined at 573 K for 3 h. The crystal type of the sample changed gradually with rising calcination temperature. The Al₂O₃ samples mainly exist as the crystal type of γ -Al₂O₃ ($2\theta=67^{\circ}, 46^{\circ}, \text{ and } 37^{\circ}$)^[17] and α -Al₂O₃ ($2\theta=43^{\circ}, 35^{\circ}, \text{ and } 57^{\circ}$)^[18,19] after AlOOH was calcined at 873 and 1473 K, respectively. This transformation of crystal structure is consistent with the report in the literature^[20].

The results of BET measurement showed that the surface areas of AlOOH, Al₂O₃-A, Al₂O₃-B, and Al₂O₃-C samples were 318, 277, 257, and 12 m² \cdot g $^{-1}$, respectively. After the calcination treatment, the surface structure and the bulk structure

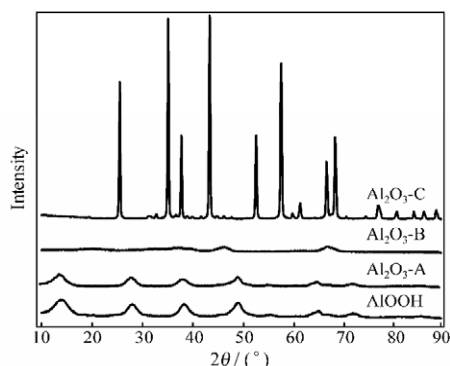


Fig.1 XRD patterns of samples for AlOOH and Al₂O₃ calcined at different temperatures

Al₂O₃-A: 573 K, Al₂O₃-B: 873 K, Al₂O₃-C: 1473 K

of the samples were reframed owing to the crystal transformation, and thus the surface area of the samples changed.

2.2 Effect of oxygen on catalytic hydrolysis activity of OCS over Al₂O₃-A at room temperature

Previous studies showed that oxygen in the reactant gases was the main factor for the catalyst poisoning in OCS hydrolysis at high temperature^[11–14]. In this study, the influence of oxygen concentration on the catalytic hydrolysis activity of OCS was investigated over the Al₂O₃-A sample at room temperature (Fig.2). In Fig.2, we can see that the hydrolysis activity of OCS declines dramatically in the initial 1 h. This decrease was mainly because of the saturated adsorption of OCS over catalyst. When oxygen exists in the reactant gases, the catalytic activity of the Al₂O₃-A sample for the OCS hydrolysis decreased evidently. 2% oxygen led to the decrease of the hydrolysis activity (represented by the conversion ratio of OCS after reacting for 3 h) from 0.549 (without oxygen) to 0.380, and the hydrolysis activity descended to 0.308 when 10% oxygen was present in the reactant gases. The sample did not change evidently after reacting in the absence of oxygen, while a thin yellow material was obviously found on the surface of catalyst after OCS reacted in the presence of oxygen. The light yellow color on the surface of catalyst faded away

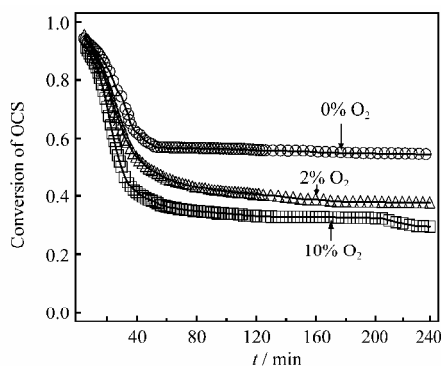


Fig.2 Effect of oxygen concentration on catalytic hydrolysis of OCS over Al₂O₃-A sample

$\phi(\text{OCS})=0.03\%$, $\phi(\text{H}_2\text{O})=0.24\%$, GHSV=2500 h⁻¹, T=298 K

after depositing for a period of time. The products of OCS hydrolysis are H₂S and CO₂. H₂S can be oxidized readily by oxygen to activated elemental sulfur.

2.3 In situ DRIFTS study of OCS catalytic hydrolysis over the Al₂O₃ sample

2.3.1 Catalytic reaction of OCS over the preoxidized Al₂O₃-A sample in a closed system

The preoxidized Al₂O₃-A sample (AlOOH calcined at 573 K for 3 h), which was pretreated in the *in situ* DRIFTS chamber, was cooled to 298 K, and then exposed to a flow rate of 100 mL·min⁻¹ 0.05% OCS + 95% O₂ at 298 K for 5 min, and then the inlet and outlet of the *in situ* DRIFTS chamber were closed. The *in situ* DRIFTS spectra for the Al₂O₃-A sample were recorded as a dynamic change with time (Fig.3). It can be seen from Fig.3 that the addition of OCS gives rise to a series of IR absorption peaks in the range of 2800–1200 cm⁻¹. The strongest absorption peaks at 2071 and 2052 cm⁻¹ can be attributed to the characteristic absorption of gas-phase OCS^[21,22]. The 2071 and 2052 cm⁻¹ bands are the R and P branches of rotational bands coupling with the antisymmetric stretching vibration spectra of OCS^[23], respectively. When the supply of OCS was stopped, the intensity of the above two peaks for OCS diminished rapidly. Meanwhile, a pair of characteristic absorption peaks of gas-phase carbon dioxide (CO₂) was observed at 2361 and 2337 cm⁻¹, and increased in intensity with time^[24,25]. Furthermore, the absorption peaks for the symmetric and antisymmetric stretching vibration of the surface HCO₃⁻ species at 1647 and 1412 cm⁻¹ also became stronger apparently^[21,24–26]. In addition, the characteristic absorption peak of the surface SO₄²⁻ species at 1354 cm⁻¹ also grew faintly in intensity^[27–29]. The generation of H₂S was detected on line by mass spectrometry (MS) during the reaction. However, no absorption peaks of gas-phase or the adsorbed H₂S were detected in the *in situ* DRIFTS. The change of the gas-phase OCS and CO₂ concentrations with time is shown in Fig.4. It can be seen that the concentration of OCS only reduced slightly with the extension of the reaction time over the

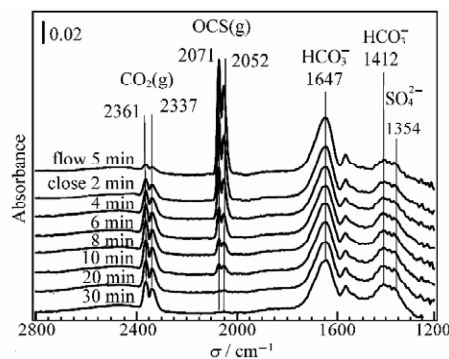


Fig.3 *In situ* DRIFTS spectra of the preoxidized Al₂O₃-A sample in closed system after exposure to reactant gases

$\phi(\text{OCS})=0.05\%$, $\phi(\text{O}_2)=10\%$, T=298 K

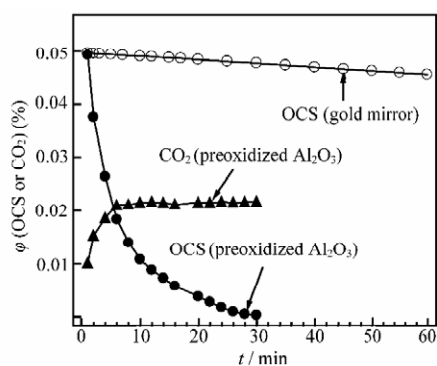


Fig.4 Concentrations of gas-phase OCS and CO₂ versus time over the preoxidized Al₂O₃-A sample or gold mirror at 298 K in closed system

surface of the reactor (a gold mirror used as a background). This indicates that the contribution of the reactor surface to the catalytic activity can be ignored. In contrast, the concentration of gaseous OCS decreased drastically with the reaction time over the surface of the Al₂O₃-A sample and diminished at about 20 min. Meanwhile, the intensity of gas-phase CO₂ reached a maximum at about 10 min. This can be ascribed to the balance between the gaseous CO₂ and the adsorbed HCO₃⁻ species on the surface. These experimental results indicated that a catalytic reaction of OCS occurred over the Al₂O₃-A sample and gas-phase CO₂, and surface HCO₃⁻ and SO₄²⁻ species were formed. However, the quantity of surface SO₄²⁻ species is very low because the amount of OCS in the *in situ* DRIFTS chamber is very limited.

2.3.2 Catalytic reaction of OCS over the preoxidized Al₂O₃-A sample in a flow system

Fig.5 shows the *in situ* DRIFTS rate spectra of the preoxidized Al₂O₃-A sample reacted in a flow rate of 100 mL·min⁻¹ 0.05% OCS + 95% O₂ at 298 K. The intensities of the absorption peaks ascribing to surface HCO₃⁻ (1639 and 1412 cm⁻¹) and SO₄²⁻ (1333 cm⁻¹) species increased with time within 2 h. It was different from Fig.3 that the peak at 1242 cm⁻¹ could be assigned to the surface HSO₃⁻ species^[30], and the intensities

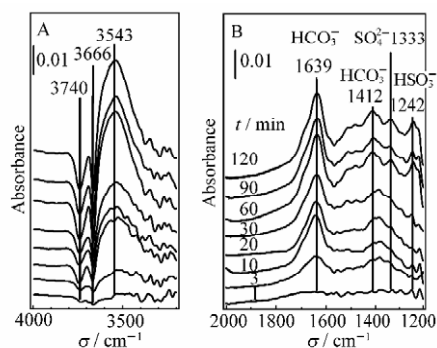


Fig.5 *In situ* DRIFTS spectra of the preoxidized Al₂O₃-A sample in flow system
φ(OCS)=0.05%, φ(O₂)=95%, T=298 K

increased with time. At the same time, in the range of 4000–3200 cm⁻¹, the consumption of surface hydroxyl (–OH) species was observed at 3740 and 3666 cm⁻¹^[31–33]. This indicates that the hydrolysis reaction of OCS is closely related to the surface –OH species on catalyst. The accumulation of a little water in flow gas on catalyst led to a strong broad band nearby 3543 cm⁻¹ (ν_{OH}), and its scissors mode (δ_{OH}) also partially contributed to the peak at 1639 cm⁻¹.

2.3.3 Catalytic reaction of OCS over the prereduced Al₂O₃-A samples in a flow system

Some other important intermediates, which will help to understand the hydrolysis process of OCS, were not detected in the above experiments owing to the high reaction activity of catalyst. Oxygen containing surface species on catalyst may play an important role in the formation of surface HSO₃⁻ and SO₄²⁻ species. It is generally believed that the prereduction of Al₂O₃ using hydrogen can reduce the surface oxygen species, and then weaken the oxidized reactivity of Al₂O₃. Therefore, we investigated the catalytic reaction of OCS over the prereduced Al₂O₃-A sample.

Fig.6 is the *in situ* DRIFTS spectra of the prereduced Al₂O₃-A sample reacted in a flow rate of 100 mL·min⁻¹ 0.05% OCS + 95% H₂ at 298 K. When compared with the oxidized system in Fig.5, the surface HCO₃⁻ species (1653 and 1390 cm⁻¹) still formed over the surface of the prereduced Al₂O₃-A sample; however, the peak intensity was considerably weaker than that in Fig.5. The consumption of surface –OH species can also be observed at 3724 and 3668 cm⁻¹. However, the production of surface HSO₃⁻ (1248 cm⁻¹) and SO₄²⁻ (1300 cm⁻¹) species reduced significantly. In contrast, a strong absorption peak appeared at 1574 cm⁻¹, which was assigned to the characteristic absorption of the surface hydrogen thiocarbonate (HSCO₂⁻) species as an intermediate of the OCS hydrolysis^[21,22,34]. The experimental results indicated that OCS was oxidized to surface HSO₃⁻ and SO₄²⁻ species *via* surface HSCO₂⁻ species over the Al₂O₃ sample. It can be deduced that further oxidation of the intermediate surface HSCO₂⁻ species

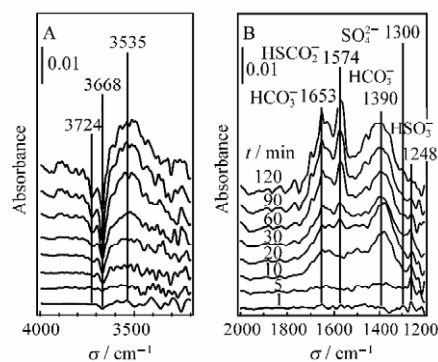


Fig.6 *In situ* DRIFTS spectra of the prereduced Al₂O₃-A sample in flow system
φ(OCS)=0.05%, φ(H₂)=95%, T=298 K

into the final product surface SO_4^{2-} species was blocked on the prereduced Al_2O_3 . As a result, the surface HSCO_2^- species was accumulated. It can be concluded that the surface oxygen species plays an important role in the catalytic reaction of OCS.

2.3.4 Catalytic reaction of OCS over the preoxidized Al_2O_3 -B and Al_2O_3 -C samples

The surface HSCO_2^- species is the product of OCS after reacting with surface $-\text{OH}$ species. Therefore, the surface $-\text{OH}$ species is probably an important active site for the hydrolysis of OCS. Considering that the different calcination temperature has a great influence on the surface $-\text{OH}$ groups on Al_2O_3 ^[18,35], the hydrolysis activities of OCS over the preoxidized samples in a closed system were investigated. Fig.7 shows the change of the gas-phase OCS concentrations with time over preoxidized Al_2O_3 samples in a closed system. It is apparent that the order of the consumption rate of OCS is $\text{Al}_2\text{O}_3\text{-A} > \text{Al}_2\text{O}_3\text{-B} > \text{Al}_2\text{O}_3\text{-C}$. Generally, it is thought that the specific surface area is an important factor that affects the reaction. However, the $\text{Al}_2\text{O}_3\text{-A}$ and $\text{Al}_2\text{O}_3\text{-B}$ samples have a similar surface area, but they have very different reaction rates. This indicates that there are other factors that affect the catalytic hydrolysis of OCS. On the other hand, the crystal types of $\text{Al}_2\text{O}_3\text{-A}$, $\text{Al}_2\text{O}_3\text{-B}$, and $\text{Al}_2\text{O}_3\text{-C}$ were transported from an amorphous structure via $\gamma\text{-Al}_2\text{O}_3$ to $\alpha\text{-Al}_2\text{O}_3$, with the specific surface area and the quantity of surface $-\text{OH}$ species decreasing, and then the catalytic reaction of OCS over Al_2O_3 was slowed down. This further illustrates that the surface $-\text{OH}$ species plays an important role in the catalytic reaction of OCS.

The above experimental results indicate that the surface $-\text{OH}$ species is the key species of the OCS catalytic hydrolysis over Al_2O_3 at room temperature. The catalytic reactions of OCS over the $\text{Al}_2\text{O}_3\text{-B}$ and $\text{Al}_2\text{O}_3\text{-C}$ samples were slowed down with the decrease of the surface $-\text{OH}$ species. It enables the observation of the catalytic reaction intermediate being possible. Fig.8 shows the *in situ* DRIFTS spectra of the preoxidized $\text{Al}_2\text{O}_3\text{-B}$ sample reacted in a flow rate of $100 \text{ mL}\cdot\text{min}^{-1}$ $0.05\% \text{ OCS} + 95\% \text{ O}_2$ at 298 K. When compared with Fig.5, the surface HCO_3^- (1653 and 1423 cm^{-1}) still

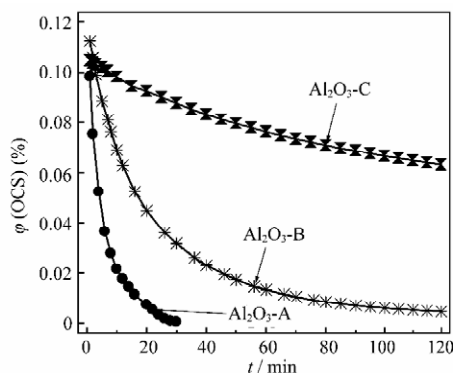


Fig.7 Concentrations of gas-phase OCS versus time over the preoxidized Al_2O_3 samples at 298 K in closed system

formed on the surface of the preoxidized $\text{Al}_2\text{O}_3\text{-B}$ sample, and the negative peaks of the surface $-\text{OH}$ species can also be observed at 3770 , 3732 , and 3683 cm^{-1} . However, the formation of surface SO_4^{2-} (1333 cm^{-1}) species was reduced significantly when compared with that of the $\text{Al}_2\text{O}_3\text{-A}$ sample. The characteristic absorption peak of surface HSCO_2^- species at 1576 cm^{-1} increased at the beginning of the reaction and then decreased. Meanwhile, the absorption peaks at 1996 and 1938 cm^{-1} owing to the physical adsorption of OCS also showed similar change^[21,34]. The surface HSCO_2^- species, which formed from the reaction of OCS with the surface $-\text{OH}$ species, was accumulated since the further oxidation to the final products (SO_4^{2-}) was inhibited significantly by the decrease of surface hydroxyl at higher pretreatment temperature.

For the $\text{Al}_2\text{O}_3\text{-C}$ sample calcined at 1473 K , the hydrolysis of OCS did not occur except for the IR absorption peak of water^[15], which indicates that the catalytic hydrolysis of OCS is extremely weak over the $\text{Al}_2\text{O}_3\text{-C}$ sample that has few surface $-\text{OH}$ species. This agrees with the results in Fig.7. These experimental results indicate that surface $-\text{OH}$ species plays a key role in the formation of the surface HSCO_2^- species for the hydrolysis of OCS, and also participates in the conversion of the surface HSCO_2^- species to the surface HSO_3^- and SO_4^{2-} species.

2.3.5 The sulfate formation of catalytic OCS over the Al_2O_3 samples

The above experiments showed that the catalytic hydrolysis of OCS occurred over the $\text{Al}_2\text{O}_3\text{-A}$ and $\text{Al}_2\text{O}_3\text{-B}$ samples under aerobic conditions at room temperature and the surface SO_4^{2-} species was formed finally. However, it is difficult to quantitatively analyze sulfate by *in situ* DRIFTS experiments; the quantitative analysis of the sulfate formed from OCS over the $\text{Al}_2\text{O}_3\text{-A}$ and $\text{Al}_2\text{O}_3\text{-B}$ samples was investigated using IC.

The quantity of sulfate formed from OCS over the $\text{Al}_2\text{O}_3\text{-A}$ and $\text{Al}_2\text{O}_3\text{-B}$ samples varies with the reaction time as shown in Fig.9. The quantity of sulfate increased rapidly at the beginning stage of the reaction and slowed down gradually after 2 h

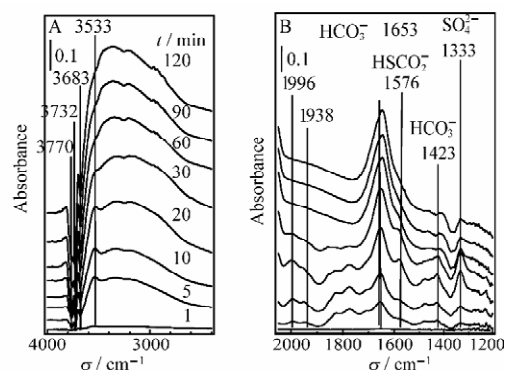


Fig.8 *In situ* DRIFTS spectra of the preoxidized $\text{Al}_2\text{O}_3\text{-B}$ sample in flow system

$\phi(\text{OCS})=0.05\%$, $\phi(\text{O}_2)=95\%$, $T=298 \text{ K}$

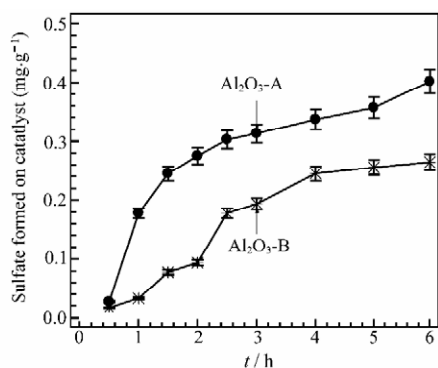


Fig.9 Sulfate formed on the preoxidized Al₂O₃-A and Al₂O₃-B samples *versus* the reaction time at 298 K

and 4 h for Al₂O₃-A and Al₂O₃-B, respectively. This indicates that the formed sulfate occupies the reactive sites on the Al₂O₃ sample. This phenomenon is consistent with that in the *in situ* DRIFTS experiments (Figs. 5B and 8B). In addition, the content of accumulated sulfate over the Al₂O₃-A sample is higher than that over the Al₂O₃-B sample, which indicates that the catalytic oxidation of OCS over the Al₂O₃-A sample is easier than that over the Al₂O₃-B sample.

2.3.6 Oxygen poisoning mechanism of the catalytic hydrolysis of OCS over Al₂O₃

On the basis of the above experimental results, we proposed the following possible oxygen poisoning mechanism for the catalytic hydrolysis of OCS over Al₂O₃ at room temperature as shown in Fig.10. OCS first reacted with the surface –OH species to form the intermediate surface HSCO₂[–] species on Al₂O₃ at room temperature. When oxygen was absent, the hydrolysis reaction of surface HSCO₂[–] species proceeded to generate H₂S and CO₂. When oxygen was present, the surface HSCO₂[–] species was converted to the surface HSO₃[–] and HCO₃[–] species by the surface oxygen species and surface –OH species at room temperature, and then surface HSO₃[–] could be further oxidized to the surface SO₄^{2–} species. On the other hand, H₂S could react with the oxygen containing surface species to generate high activity elemental sulfur. H₂S or elemental sulfur could be converted into surface SO₄^{2–} species by the surface oxygen species. When the surface oxygen species was consumed, O₂ in the gas-phase activated by the Al₂O₃ sample could supple-

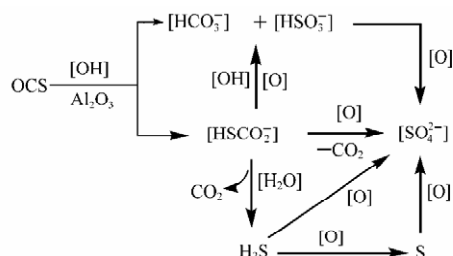


Fig.10 Oxygen poisoning mechanism of the catalytic hydrolysis of OCS over Al₂O₃ sample

ment it so that the oxidation reaction could be continued until the surface was fully covered by the surface HCO₃[–] and SO₄^{2–} species. Thus, both the surface oxygen species and the surface –OH species play important roles in the oxygen poisoning of OCS.

3 Conclusions

The main reason for the oxygen poisoning of the catalytic hydrolysis is that OCS can undergo catalytically hydrolysis on Al₂O₃ surface to produce gas-phase CO₂, elemental sulfur, and surface HCO₃[–], HSO₃[–], and SO₄^{2–} species at room temperature. The absorbed OCS can react with the surface –OH species to form the key intermediate for the catalytic hydrolysis and oxidation of OCS: the surface HSCO₂[–] species. Both the surface oxygen species and the surface –OH species play important roles in the oxygen poisoning of OCS. When the quantity of the surface –OH species was reduced (by the thermal pre-treatment of the Al₂O₃ sample) or the quantity of oxygen containing surface species was reduced (by the prereduction of the Al₂O₃ sample), the catalytic oxidation ability of Al₂O₃ for OCS was weakened. Further oxidation of the intermediate surface HSCO₂[–] species was inhibited, which can prevent the oxygen poisoning of OCS over Al₂O₃. Thus, the prereduced treatment and the reducing atmosphere in reactant gases are the available ways to restrain the OCS oxidized into the surface SO₄^{2–} species over Al₂O₃.

References

- Rhodes, C.; Riddel, S. A.; West, J.; Williams, B. P.; Hutchings, G. J. *Catal. Today*, **2000**, *59*: 443
- Watts, S. F.; Roberts, C. N. *Atmos. Environ.*, **1998**, *33*(1): 169
- Pearson, M. J. *Hydrocarbon Proc.*, **1981**, *60*(4): 131
- Liu, Z. T.; Li, Y. W.; Zhou, J. L.; Zhang, B. J. *Natural Gas Chemical Industry*, **1994**, *19*(5): 15
- Crutzen, P. J. *Geophys. Res. Lett.*, **1976**, *3*: 73
- Watts, S. F. *Atmos. Environ.*, **2000**, *34*(5): 761
- Li, X. X.; Liu, Y. X.; Wei, X. H. *Modern Chem. Industry*, **2004**, *24*(8): 19
- West, J.; Williams, B. P.; Young, N.; Rhodes, C.; Hutchings, G. J. *Catal. Comm.*, **2001**, (2): 135
- Wang, H.; Tan, S. S.; Guo, H. X. *Coal Chem. Industry*, **1991**, *56*(3): 28
- Liang, M. S.; Li, C. H.; Guo, H. X.; Xie, K. C. *Chin. J. Catal.*, **2002**, *23*(4): 357
- Fiedorow, R.; Léatuté, R.; Dalla Lana, I. G. *J. Catal.*, **1984**, *85*(2): 339
- Zhang, Q. L.; Guo, H. X. *Chin. J. Catal.*, **1988**, *9*(2): 131
- Liang, M. S.; Li, C. H.; Guo, H. X.; Xie, K. C. *J. Fuel Chem. Tech.*, **2002**, *30*(4): 347
- Lin, J. Y.; Guo, H. X.; Xie, K. C. *J. Ningxia University (Natural Science Edition)*, **2001**, *22*(2): 192
- Liu, J. F.; Yu, Y. B.; Mu, Y. J.; He, H. J. *Phys. Chem. B*, **2006**,

- 110(7): 3225
- 16 He, H. *Acta Scientiae Circumstantiae*, **2003**, **23**(2): 224
- 17 Aytam, H. P.; Akula, V.; Janmanchi, K.; Kamaraju, S. R. R.; Panja, K. R.; Gurram, K.; Niemantsverdriet, J. W. *J. Phys. Chem. B*, **2002**, **106**: 1024
- 18 Bhattacharya, I. N.; Gochhayat, P. K.; Mukherjee, P. S.; Paul, S.; Mitra, P. K. *Mater. Chem. Phys.*, **2004**, **88**: 32
- 19 Lu, H.; Sun, H.; Mao, A.; Yang, H.; Wang, H.; Hu, X. *Mater. Sci. Eng. A*, **2005**, **406**: 19
- 20 Morterra, C.; Magnacca, G. *Catal. Today*, **1996**, **27**: 497
- 21 Lavalley, J. C.; Travert, J.; Chevreau, T.; Lamotte, J.; Saur, O. *J. Chem. Soc., Chem. Commun.*, **1979**, **4**: 146
- 22 Lavalley, J. C.; Aboulayt, K.; Lion, M.; Bachelier, J.; Hebrard, J. L.; Luck, F. Symposium on NO_x and SO₂ control in stationary sources. Am. Chem. Soc. Atlanta Meeting, April 14–19, 1991: 43
- 23 Tubergen, M. J.; Lavrich, R. J.; McCargar, J. M. *J. Chem. Edu.*, **2000**, **77**: 1637
- 24 Amenomiya, Y.; Morikawa, Y.; Pleizier, G. *J. Catal.*, **1977**, **46**: 431
- 25 Nemeth, L.; Gati, G.; Gervasini, A.; Auroux, A.; Mink, G.; Pap, I. S.; Szekeley, T. *Appl. Catal.*, **1990**, **64**: 143
- 26 Molina, R.; Centeno, M. A.; Poncelet, G. *J. Phys. Chem. B*, **1999**, **103**: 6036
- 27 Saur, O.; Bensitel, M.; Mohammed Saad, A. B.; Lavalley, J. C.; Tripp, C. P.; Morrow, B. A. *J. Catal.*, **1986**, **99**: 104
- 28 Lavalley, J. C. *Catal. Today*, **1996**, **27**: 377
- 29 Meunier, F. C.; Ross, J. R. H. *Appl. Catal. B*, **2000**, **24**: 23
- 30 Sahibed-Dine, A.; Aboulayt, A.; Bensitel, M.; Mohammed Saad, A. B.; Daturi, M.; Lavalley, J. C. *J. Mol. Catal. A*, **2000**, **162**: 125
- 31 Mitchell, M. B.; Sheinker, V. N.; White, M. G. *J. Phys. Chem.*, **1996**, **100**: 7550
- 32 Peri, J. B.; Hannan, R. B. *J. Phys. Chem.*, **1960**, **64**: 1526
- 33 Peri, J. B. *J. Phys. Chem.*, **1965**, **69**: 220
- 34 Hoggan, P. E.; Aboulayt, A.; Pieplu, A.; Nortier, P.; Lavalley, J. C. *J. Catal.*, **1994**, **149**: 300
- 35 James, W. H.; William, F. B. *Thermochimica Acta*, **1996**, **288**: 179